Science Education and Application Journal (SEAJ)
Program Studi Pendidikan IPA
Universitas Islam Lamongan
http://jurnalpendidikan.unisla.ac.id/index.php/SEAJ

March, 2025. Vol. 7, No. 1,
p-ISSN: 2656-6672
e-ISSN: 2656-8365
pp.108-120

Validation of Atmospheric Instability Indices from Himawari-9 Against Radiosonde Observations

[1]Rayhan Rafi, [2]Roihan Fauzi Citra, [3]Delfiana Yoventa Buti
[1,2,3]State Collage of Meteorology, Climatology, and Geophysics
Email Correspondence: rayhan.rafi26@gmail.com

Article Info

Article History
Received: January, 24th, 2025
Revised: March, 18th, 2025
Published: March, 21st, 2025

Keywords
Himawari-9; Radiosonde Observations; Atmospheric Instability Indices; Validation

Abstract

Validation of Atmospheric Instability Indices from Himawari-9 Against Radiosonde Observations. *Remote sensing is crucial in measuring atmospheric instability by providing continuous spatial and temporal observations, often through satellite-based retrieval algorithms and numerical models. This study evaluates atmospheric instability indices derived from Numerical Weather Prediction (NWP) models using Himawari-9 satellite data. The results are compared with Radiosonde observations at the Tunggal Wulung Meteorological Observation Post, Cilacap, Central Java. The observation period includes four-time samples of Radiosonde observations identified with essential weather events. Atmospheric instability indices such as Showalter Index (SI), Lifting Index (LI), K Index (KI), Severe Weather Threat (SWEAT), and Convective Available Potential Energy (CAPE) are used to analyze the dynamics of atmospheric instability that trigger important weather events such as rain. The research method involves processing Radiosonde observation data provided by Wyoming and satellite imagery using GMLSPD software. The results of this study reveal cloud images and instability index values that explain the occurrence of essential weather events with a moderate category. Although some parameter values differ from Radiosonde data, the NWP-GSM indices from Himawari-9 are in good agreement with Radiosonde measurements for certain instability index categories. These findings suggest that Himawari-9 GSM can complement and be an alternative to Radiosonde observations by providing continuous atmospheric instability analysis, especially during periods without Radiosonde measurements. This shows its potential to improve weather monitoring and forecasting. However, further research such as high computing power, seasonal pattern analysis, and reducing errors such as parallax errors are still needed to maximize the findings.*

Citations: Rafi, R., Citra, R. F., & Buti, D. Y. (2025). Validation of Atmospheric Instability Indices from Himawari-9 Against Radiosonde Observations. Science Education and Application Journal (SEAJ), 7(1), 108-120.

INTRODUCTION

Remote sensing in meteorology, also known as atmospheric remote sensing, is a method for obtaining atmospheric information without direct contact with the observed object (Somantri, 2009) Weather satellites are not only used to monitor atmospheric conditions but also to detect and classify various types of clouds, estimate precipitation, and identify convective storm activity, aiding scientific and environmental studies (Ando et al., 2020). According to Zakir et al. (2010), the ability of weather satellites to monitor cloud distribution, rainfall, and atmospheric patterns is essential for assisting forecasters in making informed decisions about past, present, and future weather conditions.

In Indonesia, a series of Himawari satellites have been used for meteorological monitoring since the 1980s, with Himawari-9 replacing Himawari-8 in 2022. The satellite's coverage extends from the eastern part of Asia to Australia, including the Indian Ocean and the western Pacific Ocean (Kushardono, 2012). Himawari-9 has a high temporal resolution, recording spatial maps and detecting atmospheric phenomena approximately every 10 minutes (Bessho et al., 2016). The AHI (Advanced Himawari Imager) sensor instrument contains 16 observation bands, including 3 VIS (Visible) bands for daytime cloud observations, 3 NIR (Near-Infrared) bands for detecting water vapor and vegetation, and 10 IR (Infrared) bands for temperature profiling, nighttime monitoring, and weather analysis, which can be utilized according to user needs (Harjupa et al., 2021).

The Numerical Weather Prediction (NWP) method is often used to study hydrometeorological phenomena, such as severe thunderstorms, tropical cyclones, and heavy rainfall events, where cloud connectivity patterns play a crucial role (Baba et al., 2024). NWP models integrate satellite data, radiosonde measurements, and surface weather observations to simulate atmospheric dynamics and enhance the understanding of atmospheric circulation objectively (Haupt et al., 2017). The development of NWP alongside satellite advancements has improved model accuracy by providing high-resolution initial conditions, thanks to the extensive spatial and temporal coverage of satellites (Thépaut, 2003).

For upper-air observations, Radiosonde is the primary method used to measure vertical atmospheric profiles, providing data on temperature, humidity, pressure, and wind speed at different altitudes. Radiosonde is an observation system where a transmitter containing measurement sensors is attached to a helium-filled balloon to measure atmospheric parameters such as temperature, humidity, pressure, and wind speed. This balloon is launched into the air at an average speed of 100 meters per minute and typically ascends to an altitude of approximately 30 km before bursting and descending back to the surface (Wirjohamidjojo, 2006). Radiosonde data is unique and valuable for atmospheric studies. However, its availability is limited due to predefined launch schedules, which restrict data collection to specific observation hours (Athoillah et al., 2016). According to (BMG, 2006), the standard operational procedure for upper-air observations using Radiosonde involves an electronic transmitter as a sensor, flown with a 500 or 600-gram balloon twice a day, at 00:00 UTC (07:00 WIB) and 12:00 UTC (19:00 WIB).

In general, the weather parameters obtained from Radiosonde observations include temperature, dew point, wind direction and speed, and humidity. These parameters are typically presented in a vertical profile of the upper atmosphere, commonly visualized using Skew-T log-P diagrams, which meteorologists use to analyze atmospheric stability conditions (Fibriantika and Mayangwulan, 2020). These recordings provide instability data to identify the formation and growth of convective clouds, including key parameters such as Convective Available Potential Energy (CAPE) and Convective Inhibition (CIN), which are essential for assessing atmospheric instability. Radiosonde data is recorded and plotted in the form of a Skew T-log P Diagram, which visualizes atmospheric dynamics in the upper air layers (Syaifullah, 2018).

Atmospheric instability indices play a crucial role in the formation and growth patterns of clouds in the atmosphere. Instability indices, which are used on a small scale (meso-local), refer to weather systems within a range of approximately 2–200 km, typically including thunderstorms and convective cells. Some of the indices commonly analyzed include the Showalter Index (SI), Lifting Index (LI), Severe Weather Threat (SWEAT), K Index (KI), Cross Total Index, Vertical Totals Index, Totals Totals Index, Convective Available Potential Energy (CAPE), Convective Inhibition, and Bulk Richardson Number. The indicators

mentioned are lability indicators that have the potential to determine atmospheric instability. (Wirjohamidjojo and Swarinoto, 2013).

However, many previous studies, including Saragih (2020), have shown that atmospheric instability indices such as the Showalter Index (SI), Total Index (TT), Lifting Index (LI), K Index (KI), Convective Available Potential Energy (CAPE), and Severe Weather Threat (SWEAT) are sufficient to determine the current atmospheric dynamics. These indices can be derived using sounding or Radiosonde data to analyze the upper atmosphere.

Table 1. Criteria for Atmospheric Instability Indices in Convection

Instability Index	**Weak convection potential**	**Moderate convection potential**	**Strong convection potential**
Showalter Index	> 4	4 s/d -4	< (-4)
Lifted Index	>-2	-2 s/d -6	< -6
K Index	< 29	29 s/d 37	> 37
Total-totals Index	< 42	42 s/d 46	> 46
SWEAT	<135	135 s/d 239	> 329
CAPE	<1000	1000 s/d 2500	>2500

Kazumori (2018) stated that the development of NWP from Himawari has progressed rapidly, particularly in assimilating CSR (Clear Sky Radiance) data to forecast rainfall over an 11-day period. This was tested against conventional data such as Radiosonde, other satellite data (MTSAT-2) as a comparison, and pseudo-data, which represents artificial typhoon observations based on empirical approaches. The results demonstrated that the assimilation of Himawari-8 CSR data significantly improved weather analysis and forecasting, especially in capturing tropospheric moisture dynamics and extreme rainfall. A key concern is that CSR data is satellite observation data incorporated into NWP-GSM. Therefore, this study aims to contribute further research in this area.

Other studies related to the evaluation of the GSM model in Himawari satellites focus on understanding weather conditions on both global and regional scales. For example, Baba et al. (2024) analyzed the spectral model of GSM in Himawari concerning tropical cyclones. Their study, using various numerical models, demonstrated that integrating spectral schemes into the GSM model enhances forecasting skills for tropical cyclone intensity. Additionally, the spectral scheme improves the simulation of tropical variability, such as ENSO and MJO, leading to more realistic tropical cyclone structures and contributing to improved seasonal weather forecasts and reanalysis datasets.

Although these two studies do not explicitly examine instability indices in the GSM model, they highlight a common thread: several studies have explored the GSM model as a tool for analyzing spatial phenomena, yielding promising results. This study builds upon these foundations by addressing the need for further validation of Himawari-9 data, particularly in the context of instability analysis.

The objective of this study is to analyze cloud imagery during observation times, examine the values of instability indices that contribute to significant weather events (such as rainfall and storms of varying intensity), and evaluate the Numerical Weather Prediction (NWP) instability indices derived from the Himawari-9 satellite (GSM) by comparing them with vertical atmospheric profiles from Radiosonde data. The primary dataset consists of Radiosonde measurements from the Meteorological Observation Station at Wulung, Cilacap,

Central Java, while the secondary dataset includes atmospheric instability indices obtained from NWP data from the Himawari-9 satellite. By conducting this comparison, this study aims to determine whether the NWP instability indices from the Himawari-9 satellite align with or approximate the analyses derived from Radiosonde sounding data. If the results show consistency, this research could significantly benefit various sectors, including meteorological agencies (e.g., BMKG, NOAA, WMO) for enhancing weather forecast models, the aviation industry for assessing turbulence and storm risks, and disaster management teams for improving early warning systems in high-risk weather zones. Ultimately, these findings can support more accurate weather monitoring, particularly in regions and time periods lacking direct Radiosonde observations.

METHODS

The location of this study was conducted at the Meteorological Observation Station in Wulung, Cilacap Regency, Central Java Province located at a latitude of -7.643595 and a longitude of 109.035653. This location was chosen due to an operational post of Radiosonde flight station and its direct exposure to the Indian Ocean, which leads to massive cloud formation patterns and increases the potential for high rainfall. These meteorological characteristics make it a suitable site for studying atmospheric instability. The study was carried out on November 26, 2024, November 28, 2024, December 1, 2024, and December 2, 2024, at 12:00 UTC. These dates were selected based on METAR code reports indicating significant weather conditions, such as rainfall, during Radiosonde observation times. The choice of 12:00 UTC over 00:00 UTC was based on the assumption that Indonesia has a higher probability of experiencing rainfall at 12:00 UTC (19:00 WIB) compared to 00:00 UTC (07:00 WIB). This selection ensures that the study captures atmospheric instability conditions associated with significant weather events more effectively.

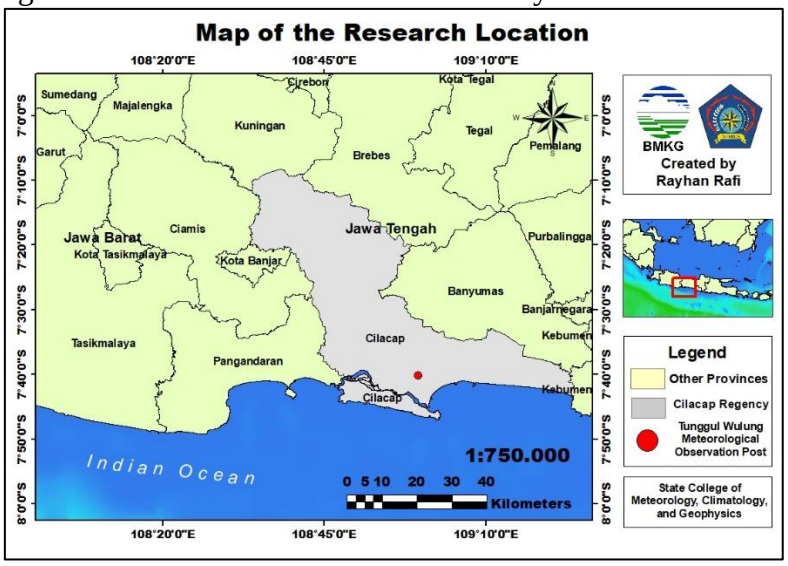

Figure 1. The location map of the Tunggul Wulung Meteorological Observation Post as the research site

This research uses a descriptive research method with a comparative study, specifically a model evaluation approach. Descriptive research is the explanation of an event, an object, a condition, or a thought that occurs with the aim of providing a factual and accurate description (Nazir, 2005).

The data collection technique begins by validating the weather type through the interpretation of the MENTAR code on the BMKG-Aviation portal data via the link https://web-aviation.bmkg.go.id/web/MENTAR_speci.php available at the ICAO location. To

ensure accuracy, inconsistencies in MENTAR reports were handled by cross-checking with SYNOP reports and Himawari-9 satellite imagery. In this study, the ICAO location "WILL" is used, which is the code for the observation station at the Tunggul Wulung Meteorological Observation Post. The purpose of this data check is to identify specific times during Radiosonde observation hours when rain or significant weather events occur. However, the data used from one observation station has limitations and The atmospheric conditions observed at a single location may not fully represent broader regional weather patterns.

Next, download the raw data from wyoming.edu in "list" type on the Radiosonde sounding data observation portal at https://weather.uwyo.edu/upperair/sounding.html by selecting the year, month, date, and observation hour as desired, then entering the station number (96805) and clicking enter. The "Skew-T" data can then be copied to obtain the vertical profile diagram of the upper air (skew T) along with the values of its instability index.

Next, download the raw data from the Himawari-9 satellite using the FileZilla software by first entering the host, username, and specific password. Download the IR channel (band 13) and GSM data into the "wis" folder. Then, process the Himawari-9 raw data using the GMLSPD64 software by clicking register, then file, selecting the downloaded files (IR and GSM channels). Zoom in on the research location, click "measure" in the function menu, select "brit" in the measure menu, input the position, click "NWP," then "GSM," and select "Vert.4 (Stab)" to determine the atmospheric instability index values such as the Showalter Index (SI), Lifting Index (LI), K Index (KI), Totals Totals Index (TT), Severe Weather Threat (SWEAT), and Convective Available Potential Energy (CAPE). To color the image, click the gray feature in the function menu, then click "sandwich" to apply color based on the cloud top temperature. The higher the cloud top temperature, the darker the color.

The final step is to compare the GSM model data with the observation data regarding the range of values. If the model values are close to or at least within the same category as those in Table 1, it can be said that the instability index values are relatively good for determining atmospheric instability conditions.

RESULTS AND DISCUSSION

Translation of MENTAR Code

The translation of the MENTAR code results is used to determine significant weather conditions that occur. This serves as supporting data to compare the analysis results of the instability index values between observation data (Radiosonde) and data from GSM Himawari-9. The time selected corresponds to the MENTAR code reporting sample that matches the Radiosonde observation hours, which are between 00:00 UTC and 12:00 UTC.

Table 2. Translation of MENTAR code for times with significant weather during Radiosonde observation hours

No	Date and Time	MENTAR Code Report	Significant Weather	Description of Significant Weather
1	26 November 2024 (12.00 UTC)	SAID33 WILL 261200 RRB MENTAR WILL 261200Z 34007KT 6000 -TSRA FEW012CB SCT014 26/26 Q1007 RMK CB OVER THE FIELD	-TSRA	During the observation, a light thunderstorm occurred.

No	Date and Time	MENTAR Code Report	Significant Weather	Description of Significant Weather
		BECMG TL1230 8000 NSW BKN013=		
2	28 November 2024 (12.00 UTC)	SAID33 WILL 281200 RRC MENTAR WILL 281200Z 00000KT 5000 -RA FEW010CB BKN015 24/23 Q1009 NOSIG RMK CB TO N=	-RA	During the observation, light rain occurred.
3	1 December 2024 (12.00 UTC)	SAID33 WILL 011200 MENTAR WILL 011200Z 34007KT 7000 -RA BKN013 26/25 Q1008 TEMPO TL1300 -TSRA FEW010CB BKN012=	-RA, TEMPO (-TSRA)	During the observation, light rain occurred, but there was a potential for light thunderstorms.
4	2 December 2024 (12.00 UTC)	SAID33 WILL 021200 MENTAR WILL 021200Z AUTO 35003KT 270V010 4600 -RA BKN100 OVC130 26/26 Q1008=	-RA	During the observation, light rain occurred.

Table 2 displays four observation time samples taken at the end of 2024 because this period is when there is a high likelihood of rainfall. Meanwhile, the observation time at 12:00 UTC corresponds to relatively frequent convection, according to the MENTAR code.

Skew T-log P Diagram Profile on Radiosonde and Himawari-9 Satellite Image along with Instability Index Values

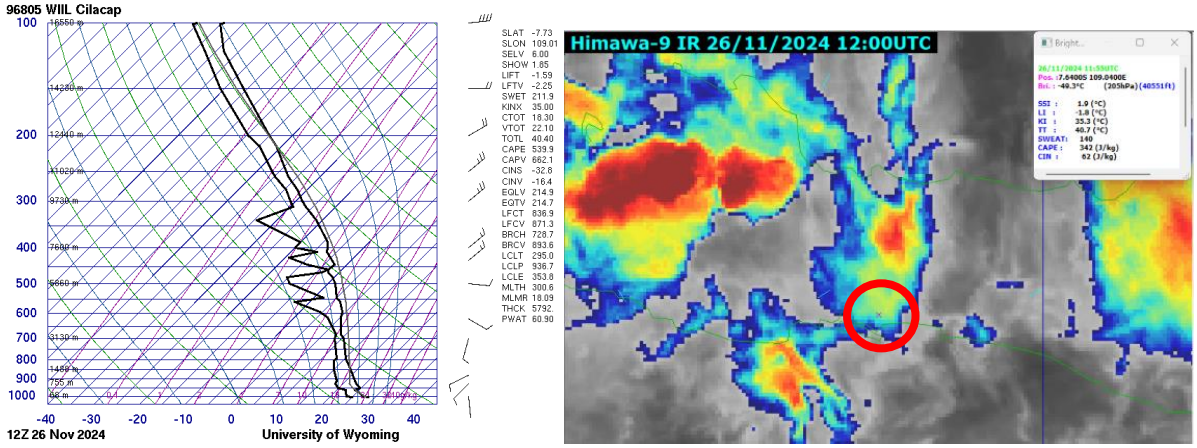

Figure 2. Skew T-log P Diagram and Himawari-9 Satellite Image along with Instability Index Values on 26 November 2024 at 12:00 UTC

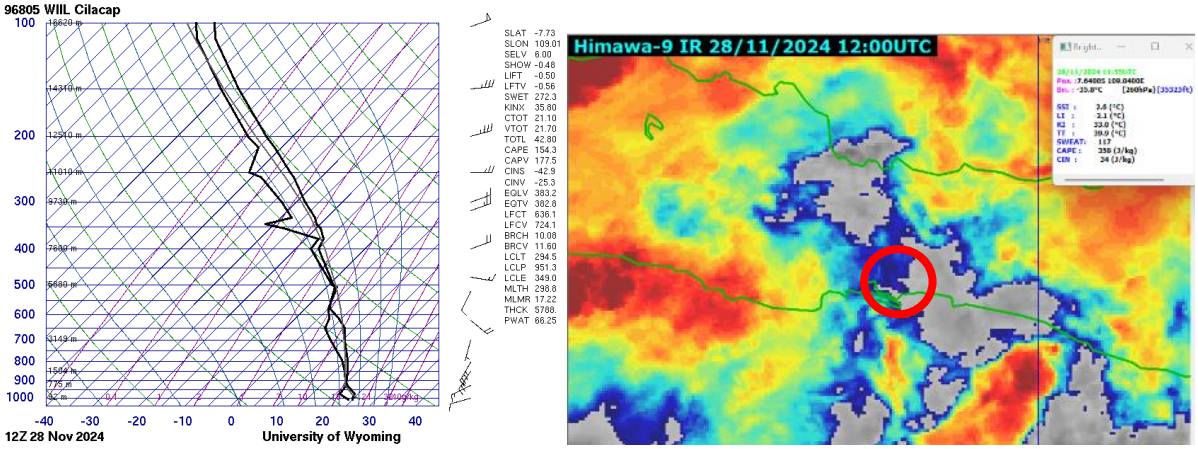

Figure 3. Skew T-log P Diagram and Himawari-9 Satellite Image along with Instability Index Values on 28 November 2024 at 12:00 UTC

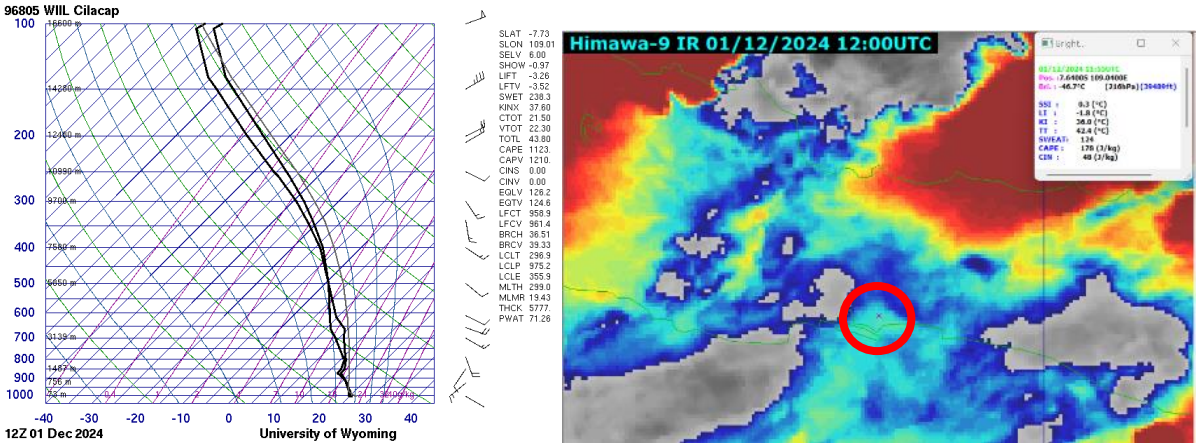

Figure 4. Skew T-log P Diagram and Himawari-9 Satellite Image along with Instability Index Values on 1 December 2024 at 12:00 UTC

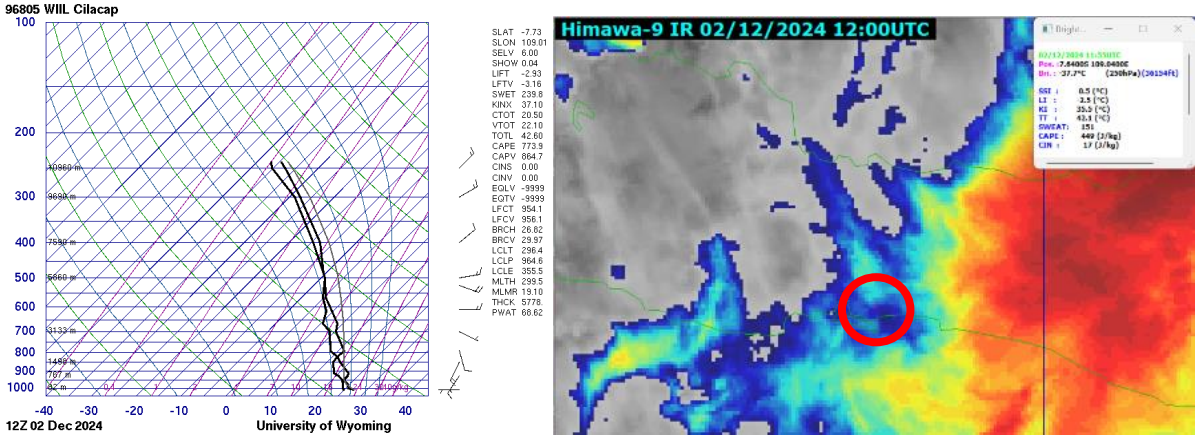

Figure 5. Skew T-log P Diagram and Himawari-9 Satellite Image along with Instability Index Values on 2 December 2024 at 12:00 UTC

Based on the four time periods taken with significant weather as shown in Figures 2, 3, 4, and 5, cloud imagery from Himawari-9 indicates the presence of convective patterns associated with potential massive cloud development. The instability index values derived from Himawari-9 imagery, such as CAPE is between 100-500 J/kg and Lifted Index values between -1 and -4, suggest moderate instability conditions. These values are generally consistent with Radiosonde observations that have an objective value of CAPE, LI, etc (The comparative of values can be seen in Table 3). This correlation indicates that Himawari-9 can reasonably

estimate atmospheric instability, aligning with observed convective activity in the cloud imagery. This is supported by the data displayed in the Skew T-log P Diagram profile, where there is a strengthening of the instability index on the parameters such as SI, LI, KI, TT, SWEAT, and CAPE in the upper atmospheric vertical profile.

Comparison of Atmospheric Instability Index Values between Radiosonde and GSM Himawari-9

The analysis of atmospheric instability index values is conducted to determine the causes of significant weather events (light rain and light thunderstorms) based on several instability index indicators. The instability indicators used include the Showalter Index (SI), Lifting Index (LI), K Index (KI), Totals Totals Index (TT), Severe Weather Threat (SWEAT), and Convective Available Potential Energy (CAPE). This chapter also provides a comparison of the values obtained from Radiosonde and GSM Himawari-9 data. From this data, The comparison of instability index values aims to evaluate the reliability of the GSM model in estimating atmospheric instability. If the results are closely aligned or at least fall within the same categorical classification (e.g., 'moderate'), it suggests that the GSM-derived instability indices from Himawari-9 can serve as an alternative to Radiosonde data. This would be particularly useful for practical meteorological applications where Radiosonde launches are not often and only at some times such as 11.00 UTC and 12.00 UTC. However, given that Radiosonde provides direct atmospheric measurements, it remains essential for the validation and calibration of satellite-based models, ensuring greater accuracy in real-time instability assessments.

Table 3. Atmospheric Instability Index Values Produced by Radiosonde and GSM Himawari-9

Date	Time	Type of Instability Index	Radiosonde Index Value	Instability Category	GSM Himawari-9 Index Value	Instability Category	Significant Weather Observed
26/11/2024	12.00 UTC	SI (°C)	1.85	Moderate	1.9	Moderate	-TSRA
		LI (°C)	-1.59	Weak	-1.8	Weak	
		KI (°C)	35	Moderate	35.3	Moderate	
		TT (°C)	40.4	Weak	40.7	Weak	
		SWEAT	211.99	Moderate	140	Moderate	
		CAPE(J/kg)	539.97	Weak	342	Weak	
28/11/2024	12.00 UTC	SI (°C)	-0.48	Moderate	2.6	Moderate	-RA
		LI (°C)	-0.5	Weak	-2.1	Moderate	
		KI (°C)	35.8	Moderate	33	Moderate	
		TT (°C)	42.8	Moderate	39.9	Weak	
		SWEAT	272.39	Strong	117	Weak	
		CAPE(J/kg)	154.31	Weak	358	Weak	
01/12/2024	12.00 UTC	SI (°C)	-0.97	Moderate	0.3	Moderate	-RA, TEMPO (-TSRA)
		LI (°C)	-3.26	Moderate	-1.8	Weak	
		KI (°C)	37.6	Strong	36	Moderate	
		TT (°C)	43.8	Moderate	42.4	Moderate	
		SWEAT	238.39	Moderate	124	Weak	
		CAPE(J/kg)	1123.07	Moderate	178	Weak	
02/12/2024	12.00 UTC	SI (°C)	0.04	Moderate	0.5	Moderate	-RA
		LI (°C)	-2.93	Moderate	-2.5	Moderate	
		KI (°C)	37.1	Strong	35.5	Moderate	
		TT (°C)	42.6	Moderate	42.1	Moderate	
		SWEAT	239.81	Strong	151	Moderate	
		CAPE(J/kg)	773.94	Weak	449	Weak	

Table 3 presents the instability index values produced by Radiosonde and GSM Himawari-9. The table shows relatively similar values with consistent category conditions. Although the categorical classifications of instability indices from Himawari-9 and Radiosonde data appear consistent, numerical differences still exist due to several factors. Radiosonde provides direct atmospheric measurements at a single location, while Himawari-9 relies on remote sensing techniques that estimate instability values based on infrared radiance. Additionally, spatial resolution differences play a role, as Radiosonde captures high-resolution vertical profiles, whereas Himawari-9 derives values from grid-based data, leading to potential averaging effects. Differences in data processing methods also contribute, as GSM utilizes numerical weather models to interpolate and estimate instability indices rather than relying on direct observations. These factors collectively explain the observed discrepancies while maintaining general categorical alignment. Rows highlighted in "yellow" indicate matching instability categories between Radiosonde and GSM Himawari-9 data, discrepancies in the unhighlighted rows may arise due to several factors. Calibration differences can cause minor variations in measured temperature and humidity, affecting instability indices. Additionally, the spatial resolution of GSM differs from Radiosonde observations, as the former provides grid-based estimations while the latter offers direct point measurements, potentially leading to inconsistencies. Environmental influences such as localized convection, wind shear, or inversions may further impact the readings. Lastly, GSM models assimilate observational data but may struggle with capturing fine-scale vertical atmospheric variations, contributing to numerical differences despite similar categorical classifications. Based on Table 3, it can be concluded that the majority of categories yield the same results despite differences in values. This indicates that GSM Himawari-9 data is relatively reliable for identifying atmospheric instability indices associated with significant weather events.

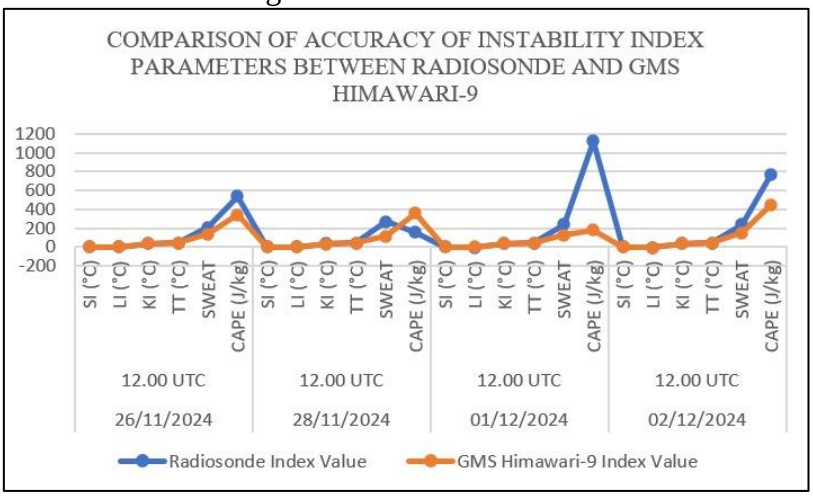

Figure 6. Comparison of the Accuracy of Radiosonde and GSM Himawari-9 Instability Index Parameters

Figure 6 shows a comparison of the accuracy of instability index parameters derived from Radiosonde observational data and GSM displayed by Himawari-9. Figure 6 compares instability indices derived from Radiosonde observations and GSM Himawari-9 data. The overall trend shows that GSM follows the Radiosonde pattern, but with lower amplitude. Notably, CAPE and SWEAT indices exhibit significant discrepancies, particularly on December 1 and December 2, 2024, where Radiosonde detects higher instability values. Conversely, SI, LI, and TT indices demonstrate closer agreement between the two datasets. These differences likely arise from the spatial averaging in GSM, which may not capture localized convective energy as effectively as direct Radiosonde observations. From this figure, it can be concluded that several parameters have similar values, such as the Showalter Index

(SI), Lifting Index (LI), K Index (KI), and Totals Totals Index (TT). Across the four time samples, these four indices exhibit close values and fall into relatively similar index categories. This differs from the values of the Severe Weather Threat (SWEAT) index and Convective Available Potential Energy (CAPE), which remain significantly different.

From this figure, it can be concluded that several indices, such as the Showalter Index (SI), Lifting Index (LI), K Index (KI), and Totals Totals Index (TT), exhibit relatively similar values between Radiosonde and GSM Himawari-9. These indices primarily depend on temperature and humidity at specific pressure levels (e.g., 850 hPa, 700 hPa, and 500 hPa), which the GSM model can capture well.

In contrast, CAPE and SWEAT indices show greater discrepancies. This is likely because they rely on the entire vertical atmospheric profile, requiring high-resolution vertical data to accurately estimate convective potential and wind shear. Since GSM employs spatial and vertical averaging, it may smooth out finer-scale atmospheric instabilities, leading to differences compared to direct Radiosonde measurements.

Expanding this study to a seasonal temporal scale would provide a more comprehensive understanding of instability index variations. Different seasons may exhibit distinct atmospheric instability patterns, which could impact the consistency between GSM Himawari-9 and Radiosonde data. By analyzing a broader timeframe, potential biases due to short-term atmospheric fluctuations could be minimized, leading to more robust conclusions

Nevertheless, all the displayed indices are still able to explain why significant weather occurred during the observation period. These findings align with Kazumori's study (2018) on the NWP CSR model, which is part of GSM, demonstrating that numerical weather models can provide reliable weather forecasts. Similarly, in terms of instability indices, our analysis shows that GSM Himawari-9 captures the general trend of atmospheric instability. However, some discrepancies, particularly in CAPE and SWEAT indices, may stem from differences in vertical resolution and convective parameterization, as also noted in Kazumori's research. The instability indices indicate the "moderate" and "strong" categories in several indices. The instability indices fall within the range of 0 to -3°C for the Showalter Index (SI), -2 to -6°C for the Lifted Index (LI), 30 to 40 for the K Index (KI), and 44 to 55 for the Total Totals Index (TT), which are classified as moderate instability. Meanwhile, values exceeding -6°C for LI and above 55 for TT indicate strong instability. These numerical thresholds provide a clearer representation of atmospheric conditions during the observation period. This suggests that cloud conditions in the atmospheric layer became unstable, as validated by the MENTAR code report presented in Table 2. However, the METAR system primarily relies on surface observations and may not fully capture instability at higher atmospheric levels. Additionally, METAR reports are subject to observer interpretation and station limitations, potentially leading to biases, especially in detecting elevated convection or instability not directly linked to surface weather phenomena.

CONCLUSION

The Cloud imagery from Himawari-9 shows variations in cloud intensity that align with the vertical wind patterns from radiosonde data, particularly in detecting the formation of convective clouds in unstable atmospheric layers. The vertical wind patterns indicate air movements that support cloud growth and aid in analyzing observation times that identify significant weather phenomena, such as rain and light storms. The instability index values obtained during the observation period, both from radiosonde and Himawari-9 GSM, such as SI, LI, KI, TT, SWEAT, and CAPE, can explain the atmospheric instability dynamics leading to significant weather events, ranging from light rain to light thunderstorm rain. Additionally, the category of instability index values between the two data sources shows that Himawari-9

GSM data provides relatively similar results. This emphasizes that GSM data can be used as a reliable alternative for analyzing atmospheric instability indices under significant weather conditions.

The use of METAR data to identify significant weather is based on the frequent association between atmospheric instability and weather phenomena such as rainfall. However, the reliability of Himawari-9 GSM data under other weather conditions has not been comprehensively tested and requires further study, particularly by considering seasonal variability. These findings offer an alternative for regions without radiosonde observations, as Himawari-9 data is widely accessible across all areas within the satellite's coverage, including Indonesia.

SUGGESTION

The authors provide suggestions for future researchers who wish to develop this study further, noting that some instability index values generated by GSM, such as SWEAT and CAPE, deviate significantly from Radiosonde observational data. This occurs due to several factors such as:

1. Parallax error correction in Himawari-9 satellite data. Satellites are typically not positioned directly above the observed object but rather at a slightly tilted or side angle. This causes objects visible in satellite imagery, such as clouds, to appear shifted from their actual positions (based on geographic coordinates on the Earth's surface). This shift is a parallax effect, which becomes more noticeable when the satellite orbits at a lower altitude or when the image perspective is sharper (Ali et al., 2021).
2. One possible approach is implementing advanced correction techniques for parallax errors in Himawari-9 data, which may affect the estimation of atmospheric instability parameters. Additionally, utilizing higher-resolution satellite data or integrating high-resolution numerical models could enhance the precision of instability index calculations, such as SWEAT and CAPE, making them more comparable to Radiosonde observational data.
3. The significant differences in SWEAT and CAPE values generated by GSM could also result from the suboptimal features of Himawari-9 GSM, as the satellite's primary concept only involves observing the cloud tops horizontally and assumes it cannot capture vertical profile changes. Therefore, for better results, data from instruments such as ground-based weather radar could be used.
4. Additionally, since atmospheric instability varies across different climates and topographies, this methodology should be tested in diverse geographical locations such as coastal vs. inland areas or tropical vs. temperate regions to assess whether Himawari-9 GSM data performs consistently under various atmospheric conditions. That's why it needs more research to find and increase the error.

ACKNOWLEDGMENTS

The authors would like to express their gratitude to the Diploma IV Meteorology Program, School of Meteorology, Climatology, and Geophysics, for the academic support, facilities, and guidance provided during this research. Special thanks are also extended to the supervising lecturer for their direction and insights, which provided the authors with profound knowledge and helped transform ideas into a proper and well-crafted written work.

REFERENCES

Ali, A., Deranadyan, G., & Sa'adah, U. (2021). Kajian awal pemanfaatan data pengindraan jauh dalam implementasi peringatan dini cuaca esktrem berbasis dampak. *Prosiding WIN-ID, 1*, 27-36.

Ando, R., Watanabe, S., Murata, K. T., dan Kunakornvong, P. (2020). Exploration of the earth's environment using "Himawari-8" data from meteorological satellites and deep learning. *Jurnal Penelitian RMUTR Bangkok*, 14(2), 1-9. https://ph02.tci-thaijo.org/index.php/rmutk/article/view/240210

Athoillah, I., Dewi, S., & Renggono, F. (2016). Perbandingan Pengukuran Radiometer dan Radiosonde pada Musim Hujan di Dramaga Bogor. *Jurnal Sains & Teknologi Modifikasi Cuaca*, *17*(2), 75. https://doi.org/10.29122/jstmc.v17i2.640

Baba, Y., Ujiie, M., Ota, Y., & Yonehara, H. (2024). Implementation and evaluation of a spectral cumulus parametrization for simulating tropical cyclones JMA-GSM. *Quarterly Journal of the Royal Meteorological Society*, *150*(761), 2045–2068. https://doi.org/10.1002/qj.4689

Bessho, K., Date, K., Hayashi, M., Ikeda, A., Imai, T., Inoue, H., Kumugai, Y., Miyakama, T., Murata, H., Ohno, T., Okuyama, A., Oyama, R., Sasaki, Y., Shimazu, Y., Shimoji, K., Sumida, Y., Suzuki, M., Taniguchi, H., Tsuchiyama, H., Yosidha, R. (2016). An Introduction to Himawari-8/9 New-Generation Geostationary Meteorological Satellites. *Journal of the Meteorological Society of Japan. Ser. II*, *94*(2), 151–183. https://doi.org/10.2151/jmsj.2016-009

BMG. (2006). Peraturan Kepala Badan Meteorologi dan Geofisika (KBMG) Nomor SK.44/ME.104/KB/BMG tahun 2006 tentang Tata Cara Tetap Pelaksanaan, Pengamatan, penyandian, dan Pelaporan Hasil Pengamatan Meteorologi Udara Atas. Jakarta, Indonesia

Fibriantika, E., & Mayangwulan, D. (2020). Analisis Spasial Indeks Stabilitas Udara di Indonesia. *Jurnal Sains & Teknologi Modifikasi Cuaca*, *21*(1), 1–12. https://doi.org/10.29122/jstmc.v21i1.4005

Harjupa, W., Ahmad, U. A., Abadi, P., Satiadi, D., & Jumianti, N . (2021). *Buku Ajar Teknologi Pengindraan Jauh Untuk Kajian Atmosfer*. Yogyakarta : Deepublish

Haupt, S. E., Jiménez, P. A., Lee, J. A., & Kosović, B. (2017). Principles of meteorology and numerical weather prediction. In *Renewable Energy Forecasting* (pp. 3–28). Elsevier. https://doi.org/10.1016/B978-0-08-100504-0.00001-9

Kazumori, M. (2018). Assimilation of Himawari-8 clear sky radiance data in JMA's global and mesoscale NWP systems. *Journal of the Meteorological Society of Japan. Ser. II*. https://doi.org/10.2151/jmsj.2018-037

Kushardono, D. (2012). Kajian satelit penginderaan jauh cuaca generasi baru Himawari 8 dan 9. *Jurnal Inderaja*, 3(5).

Nazir, M. (2005). *Metode Penelitian*. Bogor: Ghalia Indonesia

Saragih, R. W. S. (2020). Analisis Kondisi Atmosfir, Indeks Labilitas, dan Citra Satelit Saat Kejadian Puting Beliung di Pontianak Kalimantan Barat (Studi Kasus 17 Juli 2020). *Jurnal Fisika*, *10*(2), 62–71. https://doi.org/10.15294/jf.v10i2.26927

Somantri, L. (2009). Teknologi Penginderaan Jauh (Remote Sensing). *Universitas Pendidikan Indonesia*. http://file.upi.edu/Direktori/FPIPS/JUR._PEND._GEOGRAFI/132314541-LILI_SOMANTRI/makalah_Guru.pdf

Syaifullah, M. D. (2018). Analisis Kondisi Udara Atas Wilayah Indonesia dengan data Radiosonde. *Jurnal Meteorologi Dan Geofisika*, *18*(1). https://doi.org/10.31172/jmg.v18i1.268

Thépaut, J. N. 2003. Satellite data assimilation in numerical weather prediction: An overview. *In Proceedings of ECMWF Seminar on Recent Developments in Data Assimilation for Atmosphere and Ocean, ECMWF, Reading, UK* (pp. 8-12). https://www.ecmwf.int/sites/default/files/elibrary/2003/79625-satellite-data-assimilation-numerical-weather-prediction-overview_2.pdf

Wirjohamidjojo, S. (2006). *Meteorologi Praktik*. Jakarta: Badan Meteorologi Klimatologi dan Geofisika.

Wirjohamidjojo, S., & Swarinoto, Y., S. (2013). *Meteorologi Sinoptik: Analisis dan Penaksiran Hasil Analisis Cuaca Sinoptik*. Jakarta: Puslitbang BMKG.

Zakir, A., W., Sulistya, dan Khotimah. M., K. 2010. Perspektif Operasional Cuaca Tropis. Puslitbang BMKG. Jakarta.